Multi-sensor approach for multi-scale machining defect detection

Lorène Dubreuil, Yann Quinsat, Claire Lartigue

Multi-sensor approach for multi-scale machining defect detection

Lorène Dubreuil [1], Yann Quinsat [1], Claire Lartigue[1,2]

(1) : LURPA
ENS de Cachan - Université Paris Sud 11
61 avenue du Président Wilson, 94235 Cachan cedex, France
(2) : IUT Cachan
Université Paris Sud
9 avenue de la division Leclerc, 94230 Cachan, France
+33 1 47 40 29 86/+33 1 47 40 22 20

E-mail : {lorene.dubreuil, yann.quinsat, claire.lartigue}@lurpa.ens-cachan.fr

Abstract: Several measuring systems used in industries are most often used in a separated way and not efficiently. Multi-scale multi-sensor measurements are nowadays challenging to improve quality and decrease measuring time. However, this requires that each class of defects can be link with the appropriate measuring system. This paper deals with a comparative study of several measuring techniques for the measurement of multi-scale machining defects. In particular, an attention is paid to a new measuring method based on stereo-correlation along with classical measuring technique such as laser scanner, touch probe and confocal interferometry. Considering some well-known defects, the comparative study assesses the ability of each system to measure a class of defects. This study constitutes the first stage towards the definition of a multi-sensor multi-scale measuring system.

Key words: multi-sensor, digitalization, stereoscopic system, machining defect, sculptured surface

1- Introduction

Multi-scale multi-sensor measurement becomes an essential issue to improve productivity of industries. Indeed, the use of multiple systems allows simultaneous measurements, and thus a decrease in measuring time. Moreover, the use of multi-scale multi-sensors permits to linked the characteristic to be measured with the appropriate measuring system in accordance with the scale.
Many families of sensors are used in industry. Several authors offer a classification of existing measuring systems [SN1], [ST1], [CV1], [LG1]. Savio et al. [SD1] suggest a state of the art in metrology of freeform surfaces regarding the most measuring techniques used. To classify measuring systems, some authors propose comparative studies of the most common techniques used [BU1]-[ZM1]. Audfray et al. [AM1] put forward an approach of optical sensor qualification aiming at the choice of the most appropriate measuring system according to the feature to be measured. The application is limited to standardized dimensional specifications.
Several studies focus on multi-sensor measurement. Weckenmann et al. [WJ1] classifies multi-sensor measurement in three classes depending on how the sensor works (complementary, competitive or cooperative). The association of an optical sensor and a touch probe is especially explored. Chan et al. [CB1] associate a CCD camera to a touch probe in a complementary way to improve the accuracy and rapidity of the measurement, as well as Zexia et al. [ZJ1] which employ a structured-light sensor. Martinez et al. [MC1] used competitively a laser scanning and a touch probe.

Few researches address the issue of multi-scale multi-sensor measurements. Actually, manufacturing parts that have to be measured generally present deviations relative to the nominal model induced by the process. These deviations are multi-scales. Therefore, it seems necessary to adapt the measuring system with regard to its ability to locate or/and quantify deviations. However, it is not simple to directly associate the deviation to be evaluated with the appropriate measuring system. This issue is challenging.
In this context, the present paper focuses on a study of feasibility of different measuring systems to measure specific deviations induced by machining. More particularly, the addressed deviations are those obtained during a 3-axis milling operation using a ball-end cutter tool (mismatches, scallop heights, overcut).
Two different measuring systems are tested corresponding to two different measuring technologies. The first system consists of CMM equipped with a laser scanner (laser Kréon) mounted on an orientation head to increase the sensor accessibilities. The second measuring technique is the 3D-

DIC system based on stereo-vision by image correlation. This technique is relatively new in the domain of dimensional metrology.
The feasibility study is carried out thanks to a part which is defined in figure 1. The part is simple on purpose. On the one hand, classical deviations encountered during milling can be controlled, and on the other hand, the shapes are simple to measure. The part includes three different types of deviations: mismatches, scallop heights and overcuts.

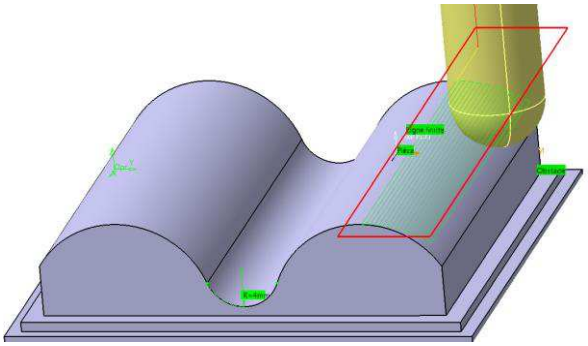

Figure 1: CAD model and example of tool path of the study part.

The test part is milled on a HSM (High Speed Machining) 3-axis milling center according a back and forth parallel plane strategy. The finishing tool used is a 5 mm ball-end cutter. With such a strategy it is possible to simply control the height of the 3D topography (scallop heights) by controlling the distance between passes. Hence, 2 different topographies are defined for the tests (Rt_1 and Rt_2). The radius of the fillet that links the two cylinders of the part is equal to 4 mm. As the tool radius is equal to 5mm, a form error is generated on the fillet corresponding to an overcut during machining (ΔZ_1). Finally, to perform the mismatch, an offset by 0.1 mm following the Z axis (tool axis) is achieved during the milling (ΔZ_2). All the deviations aforementioned are summarized in figure 2.

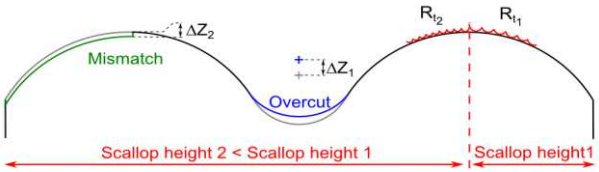

Figure 2: Diagram of the deviations applied to the test part

Whatever the technology used, the deviations are obtained by measuring a collection of 3D points on the part surfaces. It is thus necessary to present the stage of point measurement for the three measuring systems considered.
As the 3D-DIC system is new in dimensional metrology, the next section is dedicated to the description of this specific measuring method. The third section shortly details the measurement principle associated with the laser plane sensor (Kréon system). Measurement results and the feasibility study are addressed in section 4. Finally, conclusions and future works complete this study.

2- 3D-DIC system with a mesh based approach

3D-DIC system is a stereoscopic measuring technique. The difference compared to photogrammetry or stereovision relies in the way of picture pairing. Indeed, picture correlation on speckled parts is the core of the method [HR1]. Nevertheless, as for any vision system, it requires a calibration procedure to identify the parameters of the model (which is classically a model). Several calibration methods may be considered as in [LV1], [B1], [BD1].

2.1 – Stereoscopic system model and calibration

A stereoscopic system permits to build 3D points from two 2D pictures. Figure 3 puts forward this principle. As it can be seen, 2 pictures are required in order to remove the ambiguity associated with a unique picture. Due to the projective transformation, a 2D point belonging to a picture corresponds to infinity of 3D points. For instance, in figure 3, the 2D point *m* in picture 1 could be anywhere on the 3D line ΔM. With a second camera, the intersection of the two lines of a same point will give the corresponding 3D point.

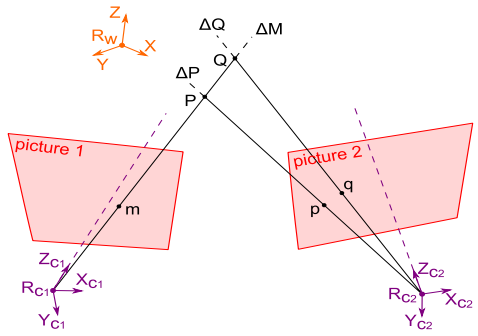

Figure 3: Stereoscopic principle with 3D point construction from two pictures.

However, a pairing technique has to be chosen to determine the same 2D points of the two pictures (*m* and *p* in the proposed example). The pairing technique used in the 3D-DIC measurement is the picture correlation.
Let us detail in the following of this section, the pinhole model, the stereoscopic model and the calibration developed to perform 3D point measurements.

2.1.1 – Pinhole model

The pinhole model is a projection perspective model which allows us to express the 3D point coordinates defined in a reference frame in the picture frame. This consists of three geometric transformations [FT1], [T1] as defined in figure 4. The transformation T between the world frame R_w and the camera frame R_c, consists of a rotation and a translation defined thanks to a homogeneous matrix (see Equation 1). The parameters associated with this transformation are called the extrinsic parameters.

$$\begin{bmatrix} X_c \\ Y_c \\ Z_c \\ 1 \end{bmatrix}_{R_c} = [T].\begin{bmatrix} X \\ Y \\ Z \\ 1 \end{bmatrix}_{R_w} = \begin{bmatrix} R_{3*3} & t \\ 0 & 1 \end{bmatrix}.\begin{bmatrix} X \\ Y \\ Z \\ 1 \end{bmatrix}_{R_w} \quad (1)$$

The second transformation P is a perspective projection of R_C in the retinal plane R_r. The last one A is an affine transformation from the picture center R_r to the picture

corner R_p.

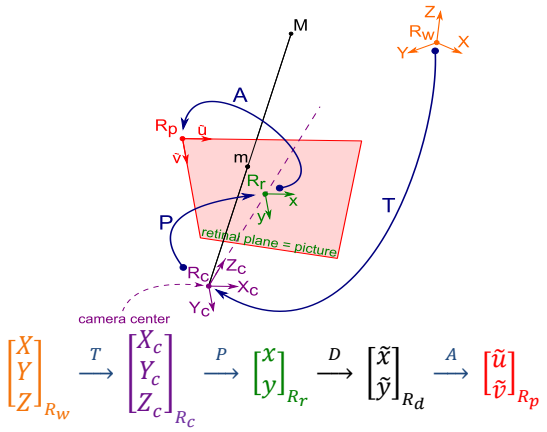

Figure 4: Pinhole model of a camera.

The parameters associated with the matrix transformations P and A are called the intrinsic parameters as for the internal parameters (focal, pixel size and number, picture center). An additional transformation D could be taken into account which corresponds to distortions of the camera. In this study, distortions are not considered. Both intrinsic and extrinsic parameters need to be identified. This is performed thanks to the calibration process.

2.1.2 – Calibration of the measuring system

The purpose of the calibration is to identify all the parameters of the pinhole model. Thus, the relationships between 3D points and picture points are assumed to be known (equation 2).

$$\begin{bmatrix}\tilde{u}\\ \tilde{v}\\ 1\end{bmatrix}_{R_p} = [APT].\begin{bmatrix}X\\ Y\\ Z\\ 1\end{bmatrix}_{R_w} \tag{2}$$

Lavest et al. [LV1] summarize all the mathematical procedure leading to camera calibration. Technically, a minimum number of points has to be known in the two frames (R_w and R_p) to achieve calibration. Several methods could be considered for this purpose. Bouguet [B1] achieves the calibration of the measuring system by shooting a well-known pattern, commonly a checkerboard pattern, in several positions. As the geometry of the pattern is supposed to be completely defined the intrinsic and extrinsic parameters can be calculated from equation 2. As this method requires numerous views of the checkerboard pattern according to different locations, acquisition time could be important.
Another method puts forward by Beaubier et al. [BD1], offers a new technique of calibration based on stereo-correlation. The particularity of this method is that the object leading to the calibration will no longer be a calibration pattern but directly the test part and its CAD model. The CAD model is more specifically a NURBS model of the test part. Hence, links between picture frames and 3D frame is virtual because the 3D frame is the CAD frame. The pairing technique is the picture correlation. The pictures shot by the left and right cameras are respectively denoted by $f(x^l)$ and $g(x^r)$, where $x^l = (\tilde{u}^l, \tilde{v}^l)$ and $x^r = (\tilde{u}^r, \tilde{v}^r)$. Conservation of the gray scale for both pictures yields equation 3.

$$f(x^l) = g(x^r) \tag{3}$$

This conservation is carried out only if the exact calibration parameters are known. As it is seldom the case, a global formulation of the sum of squared differences over the region of interest (ROI) is expressed in equation 4.

$$\tau = \int_{ROI} [f(x^l) - g(x^r)]^2 d\tilde{u}d\tilde{v} \tag{4}$$

By minimizing the correlation residual τ, calibration parameters are obtained. Contrary to the method proposed by Bouguet, this one only uses two pictures; acquisition time is thus reduced.
Another technique for extrinsic parameters identification relies on feature recognition such as lines or circles. Knowing the CAD model of a part with specified features, it is possible to associate a feature in a picture to the same feature in the CAD model. As this technique does not lead to intrinsic parameters, it only can be complementary to the previous one [B1]. The use of the two calibration methods in a complementary way permits to maximize the benefit of each one.

2.2 – 3D shape reconstruction

This section addresses the measuring method with the 3D-DIC system based on picture correlation once calibration has been performed. It is considered that the stereoscopic system is beforehand calibrated with the method proposed by Beaubier et al. [BD1].
The method proposed in the paper has drawn on the prior work developed in [BD1] but uses mesh-based approach to represent the part shapes instead of the NURBS representation previously adopted. This enlarges the possibility of shape representation in particular non-continuous in tangency surfaces can be easily described. Therefore, the parts are defined as mesh models which can be calculated from a CAD model. The minimization problem written previously in equation 4 becomes the problem linearized in equations 5 and 6 for which the unknowns correspond to the displacements of nodes of the mesh model dX.

$$\tau_{lin}(dX) = \int_{ROI} [f(x^l) - g(x^r) + (\nabla f.\delta x^l)(x^l) - (\nabla g.\delta x^r)(x^r)]^2 d\tilde{u}d\tilde{v} \tag{5}$$

$$\delta x^{l,r} = \frac{\partial x^{l,r}}{\partial X} dX \tag{6}$$

In order to respect the mesh consistency, to avoid unexpected displacements and to reduce the number of unknowns, displacements are enforced along the normal vectors of the node. In figure 5, a mesh before and after displacement is

presented. The initial mesh is pictured by nodes X_i, the final mesh is represented by nodes X_i' and the normal vectors are $\overrightarrow{n_{X_i}}$. This method also involves displacement to be evaluated only in one direction and therefore computational time is reduced.

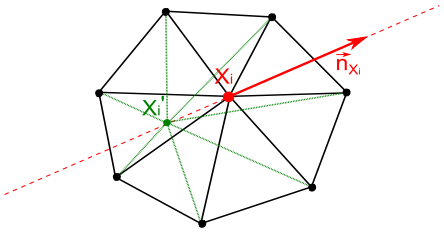

Figure 5: Principle of displacement of nodes along their normal vectors.

Considering these displacement directions, equation 6 becomes equation 7 with X_N the coordinate of nodes following its vector normal in the CAD frame.

$$\delta x^{l,r} = \frac{\partial x^{l,r}}{\partial X} \frac{\partial X}{\partial X_N} dX_N \quad (7)$$

The vector normal to a node is evaluated as the mean value of the facets surrounding the node.
As deviations are small, the assumption of small displacements of nodes is adopted. This supposes that all the normal vectors at nodes are invariant whilst the reconstruction. To improve the resolution of the equation system, integration points are added on each facet as described in figure 6.

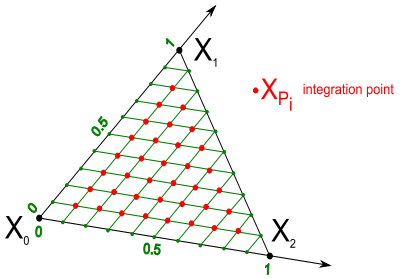

Figure 6: Discretization of a facet in integration points.

Taking into account the addition of integration points in the algorithm, equation 7 becomes equation 8 with X_P coordinates of integration points in the CAD frame.

$$\delta x^{l,r} = \frac{\partial x^{l,r}}{\partial X_p} \frac{\partial X_p}{\partial X} \frac{\partial X}{\partial X_N} dX_N \quad (8)$$

3- Laser scanning Kréon

This section introduces the measuring system also used to qualify the machined part. Laser scanners acquire a high density of point data with an acquisition time reduced. The principle of measurement is based on triangulation. Indeed, a laser plane is projected on the surface to be measured and its intersection (the profile stripe) with the surface is observed by a camera (figure 7). The coordinates of the profile stripe are determined thanks to triangulation (equation 9). The association of the laser scanner with a displacement system permits to measure the whole surface.

$$d = b * \frac{\sin\alpha . \sin\beta}{\sin(\alpha + \beta)} \quad (9)$$

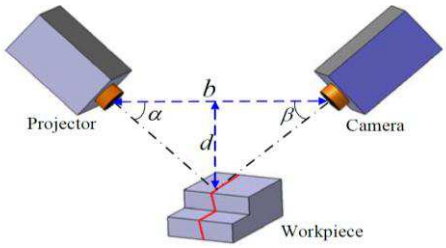

Figure 7: Triangulation principle of the laser scanner.

Nevertheless the laser scanner has several disadvantages, such as a limited viewpoint, sensitiveness to the optical conditions, digitizing noise and overlaps due to the necessity of several sensor orientations. The accuracy of the sensor is related to many factors: relative position between the sensor and the measured surface, view angle, surface conditions, etc. [AM1]. Studies have enhanced that the best conditions of scanning is obtained with a unique orientation of the laser scanner. Under these conditions, the measuring system accuracy can be assessed thanks to quality indicators: a noise of 9 µm and a trueness of 2 µm/mm [AM1].

4- Measurement of the test part and results

This section deals with the results of the comparative study conducted to evaluate the ability of each measuring system to measure the deviations previously defined (see figure 2). To define a reference, the test part has been measured with a touch probe mounted on a CMM and the sensor Stil. These measurements are chosen as references and are compared to the measurements carried out with the laser scanner Kréon and the 3D DIC system (second part of this section). Finally, the feasibility study is performed.

4.1 – First measurements of the test part

A first measurement of the part is performed to stand for the reference. Macro-defects are measured with a touch probe (Renishaw TP2 stylus), mounted on a CMM while the micro-defects are measured thanks to the Stil sensor.
Touch probe measurement is commonly used in dimensional metrology due to its high accuracy. However, its use is limited to inspection of known surfaces (prisms, cylinders, etc.) which requires lower data density. Other limitations are the accessibility of the touch probe which is impossible in areas smaller than the diameter of the tip ball.
Based on the chromatic confocal sensing technology, the sensor Stil evaluates the surface topography at micro-scale. A study conducted by Quinsat and Tournier [QT1] put forward that this sensor, used in a machine tool, is able to discriminate the surface topography evolution during machining and polishing.

The measured features acquired with the touch probe are the different cylindrical surfaces (convex and concave) presented in figure 9. The measurement of the three planes (YZ), (XZ) and (XY), allows the determination of a reference frame. This frame permits to analyze the coordinate Z of the measured data and to evaluate ΔZ_1 and ΔZ_2 in figure 2.

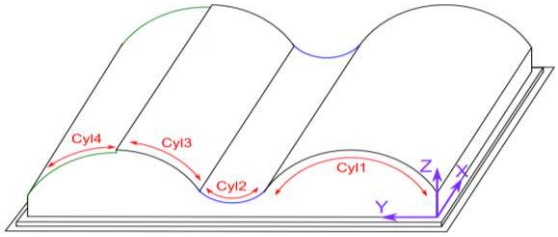

Figure 9: Features identification on the study part.

The points collected are treated thanks to the workspace "Quick Surface Reconstruction" of Catia V5. To each point cloud corresponding to a feature, a cylinder is associated via the module "Basic Surface Recognition" considering that for each one the radius and the axis are imposed. Indeed, it leads to evaluate the deviation following the Z axis corresponding to the displacement of the tool axis (see figure2). Results are displayed in table 1.

Micro-scale geometries are acquired with the STIL sensor. In particular, this sensor is well-adapted to measure the mismatch as well as the 3D topographies induced by ball-end milling. The mismatch is presented in figure 10; figure 11 illustrates an example of scallop height.

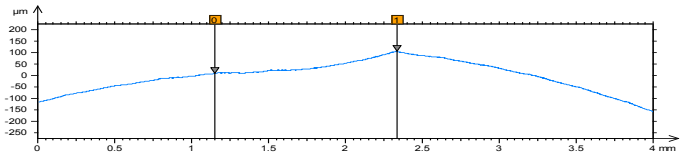

Figure 10: Mismatch (ΔZ_2) measurement with the chromatic confocal sensor Stil.

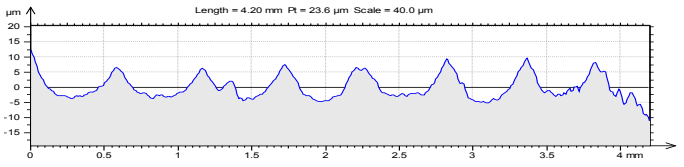

Figure 11: Scallop height (Rt_1) measurement with the chromatic confocal sensor Stil.

Mismatch (ΔZ_2) is evaluated thanks to the analysis software Mountains Map on a measured profile as in figure 10 as well as Rt_1 and Rt_2 which are evaluated directly on the extracted profile as for instance in figure 11. Results are summarized in table 1.

4.2 – Comparative study

Measurements proposed in the previous section give a reference for the errors to be evaluated. These results are compared to those obtained with the two measuring systems (Kréon and 3D-DIC). Measurements are analyzed in the same way and are displayed in table 1.

With regards to the Kréon system, it has been chosen to scan the surface with only one orientation of the laser in order to avoid overlapping errors generally appearing when using multiple sensor orientations. Based on the ICP Algorithm (Iterative Closest Point) a registration of the digitized point cloud is performed. Results from are given in figure 12 by the mapping of the deviations between the CAD model and the measured point cloud. By analyzing this mapping, overcut and mismatch are easily identified; contrary to scallop heights which are not observed.

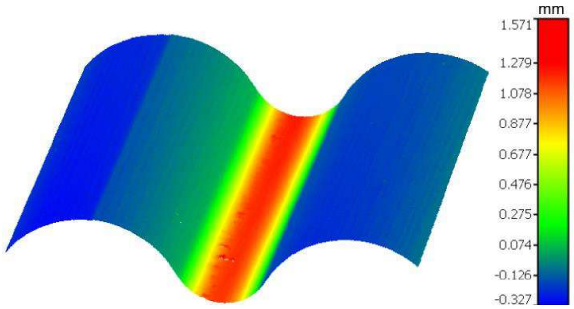

Figure 12: Mapping of deviations between the CAD model and the point cloud acquired by the Kréon after ICP registration.

Following this measurement, only the mismatch and the overcut can be thus quantified with this measuring system. With such a system, it is not possible to quantify the value of the scallop height. In table 1, the value of the deviations following Z axis obtained with the Kréon system are compared to those obtained previously with the touch probe TP2 and the sensor Stil.

To achieve 3D DIC, a black and white random pattern is projected onto the test part, and two pictures are recorded. The calibration of the stereoscopic system is achieved thanks to the CAD meshed model. In figure 14 the residual following the calibration is observed. Locations of deviations are putted forward to the places for which the residual increases. For instance, the overcut in the center of the study part is easily identifiable in figure 14.

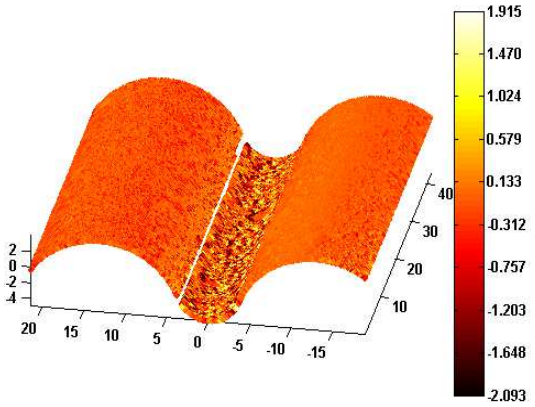

Figure 14: Residual (%) on the test part after calibration of the stereoscopic system.

Therefore, the study only concerns the overcut on the fillet (Cyl2 in figure 9). The objective is here to reconstruct the 3D-shape using the method detailed in §2.2 by node displacements. Figure 15 displayed the values of the residual on the fillet before and after node displacements with 3D-DIC. A global decrease can be observed. It is thus possible to evaluate the value of the overcut. Results relative to values of the defects obtained with 3D-DIC are summarized in table 1.
.

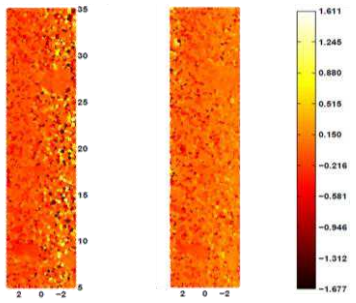

Figure 15: Residual (%) on the fillet before and after node displacements.

4.3 – Feasibility study

Table 1 summarizes all the results: those obtained with the two measuring systems (Kréon, 3D-DIC) we want to assess and the reference measurements (TP2 and Stil). After surface association to each point cloud corresponding to a feature via the module "Basic Surface Recognition" of Catia V5, ΔZ_1 and ΔZ_2 are evaluated and displayed in table 1.

Deviations	TP2	Stil	Kréon	3D-DIC
Overcut ΔZ_1 (mm)	2.077		2.059	1.934
Mismatch ΔZ_2 (mm)	0.111	0.097	0.118	
Scallop height 1 Rt_1 (µm)		11.9		
Scallop height 2 Rt_2 (µm)		5.32		

Table 1: Measurement results.

Table 1 enhances the capability of a measuring system to evaluate a class of defect. Crossed boxes put forward incompatible couples (defect/measuring system). Concerning the crossed boxes of the Kréon ant the 3D-DIC, the amplitude of the defects is of the same order as the measurement noise. The touch probe is not able to acquire surface topography. Finally, the measuring range of the sensor Stil is smaller than the size of the overcut ΔZ_1.

As might be expected, only the sensor Stil is able to detect micro-defects. Therefore, it remains the measuring system the most adapted to evaluate 3D topographies.
The system Kréon turns out to be a good solution to measure macro-defects within a large range. Indeed, results obtained with such a system a comparable to those obtained with the TP2 reference system for the overcut (of 2 mm) as well as for the mismatch (of 0.1 mm). This makes the choice of this sensor particularly relevant for this class of defects considering acquisition time and the high density of the acquired points.
The 3D-DIC measuring system only provides a result for the overcut defect, but the value remains distant from the reference value. This method needs to be improved in future works to be usable to quantify defects with a better accuracy.
However, this method provides a very smart, simple and fast method to locate macro-defects by an analysis of the residual as shown in figure 14. Therefore, once the defect is located, another system (such as TP2 or Kréon) more accurate can be used in a complementary way to quantify the value of the defect.

6- Conclusions and future works

The aim of the paper was to study the feasibility of measuring systems to measure specific defects. The study is carried out on a test part including classical defects encountered during milling (mismatch, form error, scallop height), with the objective of linking the characteristic to be measured with the appropriate measuring system. The study addressed to particular system: a commonly used laser-plane scanner Kréon, and a new system, 3D-DIC, based on stereo-correlation,
Results have highlighted that the system Kréon is the most efficient measuring system for the majority of the macro-defects. On the other hand, 3D-DIC seems to be useful to locate deviations on a part. Indeed, this study shows that deviations lower than 0.1 mm cannot be identifiable due to high noise measurement, contrary to larger deviations which are easily locate but not yet quantifiable. As expected, micro-defects are only measurable thanks to appropriate system to micro-geometry measurements such as the Stil sensor. This study enhanced the need of complementary multi-system measurements within a multi-scale multi-sensor context.
In the aftermath of this study, a multi-scale multi-sensor measuring system could be imagined. A choice on the way of how the sensor works [WJ1], will have to be established, to carry out an efficient multi-scale multi-sensor measuring system.

7- References

[AM1] Audfray, N., Mehdi-Souzani, C., and Lartigue, C. (2012). Qualification et performances des systèmes de mesure optiques : Qualipso.

[B1] Bouguet, J.-Y. (2010). Camera calibration toolbox for matlab.http://www.vision.caltech.edu/bouguetj/calib_doc/index.html

[BD1] B. Beaubier, J.-E. Dufour, F. Hild, S. Roux, S. Lavernhe and K. Lavernhe-Taillard. (2013). CAD-based calibration and shape measurement with StereoDIC. Experimental Mechanics

[BU1] Basilio Ramos Barbero and Elena Santos Ureta. Comparative study of different digitization techniques and their accuracy. Computer-Aided Design, 43(2):188 – 206, 2011.

[CB1] Chan, V., Bradley, C., and Vickers, G. (2001). A multi-sensor approach to automating coordinate measuring

machine-based reverse engineering. Computers in Industry, 44(2):105 – 115.

[CV1] Cuypers, W., Gestel, N. V., Voet, A., Kruth, J.-P., Mingneau, J., and Bleys, P. (2009). Optical measurement techniques for mobile and large-scale dimensional metrology. Optics and Lasers in Engineering, 47(34):292 – 300.

[HR1] F. Hild and S. Roux. Digital image correlation. In P. Rastogi and E. (eds) Hack, editors, Optical Methods for Solid Mechanics. A full-Fild Approach. Wiley-VCH, Weinheim (Germany), 2012.

[FT1] Faugeras O, Toscani G (1987), Camera calibration for 3D computer Vision. International Workshop on Machine Vision and Machine Intelligence 240-247.

[LG1] Yadong Li and Peihua Gu. Free-form surface inspection techniques state of the art review. Computer-Aided Design, 36(13):1395 – 1417, 2004.

[LV1] Lavest, J.-M., Viala, M., and Dhome, M. (1999). Quelle précision pour une mire d'étalonnage ?

[MC1] Martinez, S., Cuesta, E., Barreiro, J., and Alvarez, B. (2010). Analysis of laser scanning and strategies for dimensional and geometrical control. The International Journal of Advanced Manufacturing Technology, 46(5-8):621–629.

[QT1] Quinsat, Y. and Tournier, C. (2012). In situ non-contact measurements of surface roughness. Precision Engineering, 36(1):97 – 103.

[SD1] Savio, E., Chiffre, L. D., and Schmitt, R. (2007). Metrology of freeform shaped parts. {CIRP} Annals - Manufacturing Technology, 56(2):810 – 835.

[SN1] Schwenke, H., Neuschaefer-Rube, U., Pfeifer, T., and Kunzmann, H. (2002). Optical methods for dimensional metrology in production engineering. {CIRP} Annals - Manufacturing Technology, 51(2):685 – 699.

[ST1] Sansoni, G., Trebeschi, M., and Docchio, F. (2009). State-of-the-art and applications of 3d imaging sensors in industry, cultural heritage, medicine, and criminal investigation. Sensors, 9(1):568–601.

[T1] Tsai, R.Y. (1986). An Efficient and Accurate Camera Calibration Technique for 3D Machine Vision. Proceedings of IEEE Conference on Computer Vision and Pattern Recognition, Miami Beach, FL, pp. 364-374.

[WJ1] Weckenmann, A., Jiang, X., Sommer, K.-D., Neuschaefer-Rube, U., Seewig, J., Shaw, L., and Estler, T. (2009). Multisensor data fusion in dimensional metrology. {CIRP} Annals - Manufacturing Technology, 58(2):701 – 721.

[ZJ1] Zexiao, X., Jianguo, W., and Qiumei, Z. (2005). Complete 3d measurement in reverse engineering using a multi-probe system. International Journal of Machine Tools and Manufacture, 45(1213):1474 – 1486.